Journal of Engineering Mathematics **30:** 587–601, 1996.
© 1996 *Kluwer Academic Publishers. Printed in the Netherlands.*

Inviscid Fluid Flow Around a Submerged Circular Cylinder Induced by Free-surface Travelling Waves

N. RILEY and B. YAN
School of Mathematics, University of East Anglia, Norwich, NR4 7TJ.

Received 3 May 1995; accepted in revised form 6 December 1995

Abstract. We consider the fluid flow induced when free-surface travelling waves pass over a submerged circular cylinder. Perturbation methods are used to formulate a sequence of potential problems that are solved using a Boundary Element method. Favourable comparison is made, where possible, with earlier work. Attention is focused, primarily, upon the time-averaged flow about the cylinder.

1. Introduction

In this paper we consider the flow of an inviscid, incompressible fluid when monochromatic free-surface waves propagate over a submerged circular cylinder whose generators are perpendicular to the wave crests. This problem has been previously studied, and several interesting and important results have emerged. At leading order in wave amplitude Dean [1] showed that there is no reflection of the incident waves. His method, based on a conformal mapping technique, is not suitable if details of the flow field are required. Ursell [2] subsequently presented a complete solution of the problem using a series of multipole potentials. The leading-order potential flow for the case in which the cylinder is well submerged can be obtained in closed form using Milne-Thompson's circle theorem, see Chaplin [3]. In a later development Vada [4] obtained, numerically, the first and second-order diffraction potentials using a method based on Green's second identity and a Green's function given by Wehausen and Laitone [5]. His results showed, *inter alia*, that, within the numerical accuracy of his method, Dean's result of zero reflection coefficient extends to the second order also. This particular point was subsequently addressed by McIver and McIver [6], and Wu [7]. Each show how the second-order reflection coefficient R_2 may be expressed in terms of the first-order potential; McIver and McIver go on to show analytically, and so unequivocally, that $R_2 = 0$, whilst Wu [7] achieves this result numerically. This vanishing of the second-order reflection coefficient was also anticipated earlier in the experiments of Chaplin [8].

Our approach to the title problem is a numerical one, using the Boundary Element method based upon Green's second identity and the fundamental solution of Laplace's equation. In this way we obtain the complete solution up to second order, including the time-independent contribution to the solution at second order. It is this term, on which we focus most attention, that allows time-averaged properties of the flow field to be obtained. We pay particular attention to the streaming, or time-averaged, flow close to the cylinder surface and note the qualitative changes in this that take place as the cylinder depth and/or wave number change. We also show that, on average, the free surface directly over the cylinder is depressed. A favourable comparison is made with the work of Vada [4] for the unsteady flow component

and, within the accuracy of our numerical technique, there is no reflection at the second order, in accordance with the results of McIver and McIver [6] and Wu [7].

The plan of the paper is as follows. In the next section we introduce expansions in powers of the wave amplitude, and, using perturbation techniques, derive boundary-value, potential, problems for each term in our expansion of the potential. Section 3 is devoted to a discussion of our numerical technique, and the results are presented in section 4.

2. Governing equations

We consider the flow that arises when two-dimensional waves at the free surface of an incompressible, inviscid fluid of infinite depth propagate over a submerged circular cylinder; the wave crests are parallel to the generators of the cylinder. If a is the radius of the cylinder, A the amplitude of the incident waves whose frequency is ω, and g the acceleration due to gravity, we define dimensionless quantities as follows

$$\left.\begin{aligned} &x = x'/a, \quad y = y'/a, \ \epsilon = A/a, \quad h = H/a, \\ &k = a\omega^2/g, \ t = \omega t', \quad \eta = \eta'/a, \quad \phi = \phi'/\omega a^2 \end{aligned}\right\}. \tag{1}$$

In (1) x', y' are Cartesian co-ordinates whose origin is at the centre of the cylinder with y' measured vertically upwards, t' is time, H is the depth of the centre of the cylinder below the undisturbed free surface and η' its elevation above it; ϕ' is the velocity potential of the flow, assumed irrotational.

The flow under consideration is governed by Laplace's equation

$$\nabla^2\phi = 0, \tag{2}$$

with boundary conditions at the free surface, derived from the kinematic and dynamic boundary conditions at the free surface respectively as

$$\frac{\partial\eta}{\partial t} + \frac{\partial\phi}{\partial x}\frac{\partial\eta}{\partial x} = \frac{\partial\phi}{\partial y}, \tag{3}$$

$$\eta(x,t) = -k\left[\frac{\partial\phi}{\partial t} + \frac{1}{2}\left\{\left(\frac{\partial\phi}{\partial x}\right)^2 + \left(\frac{\partial\phi}{\partial y}\right)^2\right\}\right]. \tag{4}$$

Under the assumption that $\epsilon \ll 1$ we now develop a solution in the classical form

$$\phi = \epsilon\phi^{(1)} + \epsilon^2\phi^{(2)} + \cdots, \tag{5}$$

$$\eta = \epsilon\eta^{(1)} + \epsilon^2\eta^{(2)} + \cdots. \tag{6}$$

If we substitute (5) in (2), then, since the equation is linear, each term $\phi^{(i)}$ satisfies Laplace's equation. Consider next the free-surface conditions (3) and (4). Not only are these nonlinear, but are applied at a surface whose position is unknown *a priori*. We substitute the expansions (5) and (6) in (3) and (4); simultaneously we transfer the boundary condition from the exact free surface to its mean position $y = h$ by expanding the potential and its derivatives as Taylor

series. Coefficients of like powers of ϵ then yield boundary conditions for the successive terms of our expansions. From (4) the terms $O(\epsilon)$, $O(\epsilon^2)$ give, respectively,

$$\left.\begin{aligned} \eta^{(1)} &= -k\left(\frac{\partial\phi^{(1)}}{\partial t}\right), \\ \eta^{(2)} &= -k\left[\frac{\partial\phi^{(2)}}{\partial t} - k\,\frac{\partial\phi^{(1)}}{\partial t}\,\frac{\partial^2\phi^{(1)}}{\partial y\,\partial t} + \frac{1}{2}\left\{\left(\frac{\partial\phi^{(1)}}{\partial x}\right)^2 + \left(\frac{\partial\phi^{(1)}}{\partial y}\right)^2\right\}\right]_{y=h} \end{aligned}\right\}. \tag{7}$$

Carrying out the same procedure with (3), and using (7) to eliminate $\eta^{(1)}, \eta^{(2)}$, we have the conditions for $\phi^{(1)}$ and $\phi^{(2)}$ as

$$k\,\frac{\partial^2\phi^{(1)}}{\partial t^2} + \frac{\partial\phi^{(1)}}{\partial y} = 0, \tag{8}$$

$$k\,\frac{\partial^2\phi^{(2)}}{\partial t^2} + \frac{\partial\phi^{(2)}}{\partial y} = k\,\frac{\partial\phi^{(1)}}{\partial t}\left(k\,\frac{\partial^3\phi^{(1)}}{\partial y\,\partial t^2} + \frac{\partial^2\phi^{(1)}}{\partial y^2}\right) - 2k\left(\frac{\partial\phi^{(1)}}{\partial x}\,\frac{\partial^2\phi^{(1)}}{\partial x\,\partial t} + \frac{\partial\phi^{(1)}}{\partial y}\,\frac{\partial^2\phi^{(1)}}{\partial y\,\partial t}\right), \tag{9}$$

where all terms in (8) and (9) are evaluated at $y = h$.

We now write $\phi^{(1)}, \phi^{(2)}$ as

$$\phi^{(1)} = \bar{\phi}_{11}\cos(t) + \bar{\phi}_{12}\sin(t) = (\phi_{01} + \phi_{11})\cos(t) + (\phi_{02} + \phi_{12})\sin(t), \tag{10}$$

$$\phi^{(2)} = \phi_{20} + \phi_{21}\cos(2t) + \phi_{22}\sin(2t), \tag{11}$$

where $\phi_{ij} = \phi_{ij}(x, y)$. In equation (10) the incident wave is represented as

$$\phi_{01}\cos(t) + \phi_{02}\sin(t) = -\frac{1}{k}\,e^{k(y-h)}\cos(kx - t) = \phi_0 \quad \text{say.} \tag{12}$$

If we now substitute (10) to (12) in (8) and (9), the conditions at $y = h$ to be satisfied by the coefficient functions in (10) and (11) are

$$\frac{\partial\phi_{1j}}{\partial y} = k\phi_{1j}, \quad j = 1, 2 \tag{13}$$

$$\frac{\partial\phi_{20}}{\partial y} = f_{20}, \tag{14}$$

$$\frac{\partial\phi_{2j}}{\partial y} = 4k\phi_{2j} + f_{2j}, \quad j = 1, 2 \tag{15}$$

where

$$f_{20} = -\frac{k}{2}\left(\frac{\partial^2\bar{\phi}_{11}}{\partial x^2}\bar{\phi}_{12} - \frac{\partial^2\bar{\phi}_{12}}{\partial x^2}\bar{\phi}_{11}\right)_{y=h}, \tag{16}$$

$$f_{21} = -\frac{k}{2}\left(4\frac{\partial\bar{\phi}_{11}}{\partial x}\frac{\partial\bar{\phi}_{12}}{\partial x} + 6k^2\bar{\phi}_{11}\bar{\phi}_{12} + \frac{\partial^2\bar{\phi}_{11}}{\partial x^2}\bar{\phi}_{12} + \frac{\partial^2\bar{\phi}_{12}}{\partial x^2}\bar{\phi}_{11}\right)_{y=h}, \tag{17}$$

$$f_{22} = -\frac{k}{2}\left[2\left\{\left(\frac{\partial\bar{\phi}_{12}}{\partial x}\right)^2 - \left(\frac{\partial\bar{\phi}_{11}}{\partial x}\right)^2\right\} + 3k^2(\bar{\phi}_{12}^2 - \bar{\phi}_{11}^2) + \frac{\partial^2\bar{\phi}_{12}}{\partial x^2}\bar{\phi}_{12} - \frac{\partial^2\bar{\phi}_{11}}{\partial x^2}\bar{\phi}_{11}\right]_{y=h}. \tag{18}$$

The boundary-value problems for the unknown coefficient functions in (10) and (11) may now be stated as follows. At $O(\epsilon)$ we have

$$\nabla^2\phi_{1j} = 0, \; j = 1, 2, \tag{19}$$

subject to the free-surface boundary conditions (13) together with

$$\frac{\partial\phi_{1j}}{\partial r} = -\frac{\partial\phi_{0j}}{\partial r} \quad \text{on} \quad r = 1, \quad j = 1, 2, \tag{20}$$

where $r = (x^2 + y^2)^{1/2}$,

$$\frac{\partial\phi_{1j}}{\partial y} \to 0 \quad \text{as } y \to -\infty, \quad j = 1, 2 \tag{21}$$

and the radiation conditions

$$\left.\begin{aligned} &\frac{\partial\phi_{11}}{\partial x} + k\phi_{12}, \quad \frac{\partial\phi_{12}}{\partial x} - k\phi_{11} \to 0 \quad \text{as } x \to +\infty, \\ &\frac{\partial\phi_{11}}{\partial x} - k\phi_{12}, \quad \frac{\partial\phi_{12}}{\partial x} + k\phi_{11} \to 0 \quad \text{as } x \to -\infty. \end{aligned}\right\} \tag{22}$$

Turning next to the terms $O(\epsilon^2)$ we have

$$\nabla^2\phi_{2j} = 0, \quad j = 0, 1, 2, \tag{23}$$

subject to the free-surface boundary conditions (14), (15) at $y = h$ together with

$$\left.\begin{aligned} &\frac{\partial\phi_{2j}}{\partial r} = 0 \text{ on } r = 1, \qquad j = 0, 1, 2 \\ &\frac{\partial\phi_{2j}}{\partial y} = 0 \text{ as } y \to -\infty, \quad j = 0, 1, 2, \end{aligned}\right\} \tag{24}$$

and the radiation conditions

$$\frac{\partial\phi_{21}}{\partial x} + 4k\phi_{22}, \quad \frac{\partial\phi_{22}}{\partial x} - 4k\phi_{21} \to 0 \quad \text{as } x \to +\infty, \tag{25}$$

$$\frac{\partial\phi_{21}}{\partial x} - 4k\phi_{22}, \quad \frac{\partial\phi_{22}}{\partial x} + 4k\phi_{21} \to 0 \quad \text{as } x \to -\infty. \tag{26}$$

In (26) the first-order reflection coefficient, R_1, has been set to zero, as determined initially by Dean [1]. A further conditions, on ϕ_{20}, is required as $x \to \pm\infty$. We note that as $x \to -\infty$, $\phi^{(1)} \to \phi_0$, and that as $x \to +\infty$, $\phi^{(1)}$ will be of the form ϕ_0, but incorporating a phase shift. This shows that f_{20} in (14) has the property $f_{20} \to 0$ as $x \to \pm\infty$ and this in turn leads us to the condition

$$\frac{\partial\phi_{20}}{\partial x} \to 0, \quad \text{as } x \to \pm\infty. \tag{27}$$

Finally, we note that the free-surface shape is given by

$$\eta(x,t) = \epsilon(\eta_{11}\cos(t) + \eta_{12}\sin(t)) + \epsilon^2(\eta_{20} + \eta_{21}\cos(2t) + \eta_{22}\sin(2t)) + \cdots, \tag{28}$$

where

$$\left.\begin{aligned} \eta_{11} &= -k\bar{\phi}_{12} = (\sin(kx) - k\phi_{12})_{y=h}, \\ \eta_{12} &= k\bar{\phi}_{11} = (k\phi_{11} - \cos(kx))_{y=h}, \end{aligned}\right\} \tag{29}$$

and

$$\left.\begin{aligned} \eta_{20} &= -\frac{1}{4}k\left\{\left(\frac{\partial\bar{\phi}_{11}}{\partial x}\right)^2 + \left(\frac{\partial\bar{\phi}_{12}}{\partial x}\right)^2 - k^2(\bar{\phi}_{11}^2 + \bar{\phi}_{12}^2)\right\}, \\ \eta_{21} &= -k\left[2\phi_{22} + \frac{3}{4}k^2(\bar{\phi}_{11}^2 - \bar{\phi}_{12}^2) + \frac{1}{4}\left\{\left(\frac{\partial\bar{\phi}_{11}}{\partial x}\right)^2 - \left(\frac{\partial\bar{\phi}_{12}}{\partial x}\right)^2\right\}\right]_{y=h}, \\ \eta_{22} &= -k\left(-2\phi_{21} + \frac{3}{2}k^2\bar{\phi}_{11}\bar{\phi}_{12} + \frac{1}{2}\frac{\partial\bar{\phi}_{11}}{\partial x}\frac{\partial\bar{\phi}_{12}}{\partial x}\right)_{y=h}. \end{aligned}\right\} \tag{30}$$

3. Numerical technique

To solve the Laplace equation for the potentials ϕ_{ij} we adopt a Boundary Element method. Alternative numerical methods for free-surface flows are outlined by Yeung [9]. With reference to Figure 1, the solution domain, Ω say, bounded by $\partial\Omega$, is the region outside the cylinder and bounded by $x = x_\ell, x = x_r, y = y_d$ and $y = h$. Since the flow is of infinite depth, and the upstream and downstream boundary conditions are applied at $x = \pm\infty$, we must ensure that the values of x_ℓ, x_r and y_d are taken to be sufficiently large.

From Green's second identity we have, with $\mathbf{n}$ the outward unit normal to $\partial\Omega$,

$$\begin{aligned} &\int_\Omega (\phi_{ij}\nabla^2\lambda - \lambda\nabla^2\phi_{ij})\mathrm{d}\Omega \\ &\quad = \int_{\partial\Omega}\left(\phi_{ij}\frac{\partial\lambda}{\partial n} - \lambda\frac{\partial\phi_{ij}}{\partial n}\right)\mathrm{d}s, \quad i = 1, j = 1,2; \quad i = 2, j = 0,1,2, \end{aligned} \tag{31}$$

and we choose, for λ, the fundamental solution of the Laplace equation

$$\lambda(p,q) = \log|p - q|, \quad p \in \Omega \cup \partial\Omega, \quad q \in \partial\Omega. \tag{32}$$

We remark at this point that in using (31) Vada [4] chooses a Green's function that has been derived for problems of this type by Wehausen and Laitone [5]. But, as he notes, his approach does not, apparently, allow him to find the time-independent part of the second-order potential ϕ_{20}. We may now write (31) as

$$-\mu(p)\phi_{ij}(p) + \int_{\partial\Omega}\phi_{ij}(q)\frac{\partial\lambda(p,q)}{\partial n}\mathrm{d}s = \int_{\partial\Omega}\lambda(p,q)\frac{\partial\phi_{ij}(q)}{\partial n}\mathrm{d}s, \tag{33}$$

where

$$\mu(p) = \begin{cases} 2\pi & \text{if } p \in \Omega, \\ \pi & \text{if } p \in \partial\Omega. \end{cases} \tag{34}$$

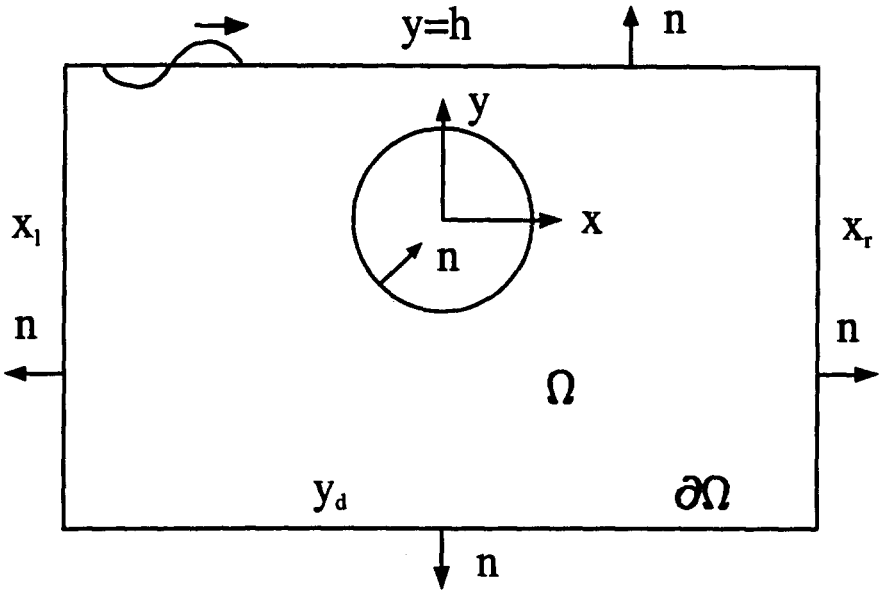

Figure 1. Definition sketch.

The boundary $\partial\Omega$ is now subdivided into a total of N straight-line elements $\partial\Omega^m, m = 1, 2, \ldots N$. On each element we approximate ϕ_{ij} by a constant value ϕ_{ij}^m and we note that $\partial\phi_{ij}/\partial n$ is known, or can be expressed in terms of $\phi_{k\ell}$, as for example in (13), (16), (22), (25) and (26). The integration over each element may now be completed analytically, and for each order in our solution scheme we have coupled linear systems of equations for ϕ_{1j} and $\phi_{2j}, j = 1, 2$ which may be written as

$$\mathbf{E}\Phi_{ij} = \mathbf{G}\mathbf{B}_{ij}(\Phi_{ij}, \Phi_{i\ell}), \quad i, j = 1, 2, \quad \ell = 1, 2, \ell \neq j, \tag{35}$$

where Φ_{ij} is the vector with elements ϕ_{ij}^m, $\mathbf{E}$, $\mathbf{G}$ are $N \times N$ matrices which depend only upon the geometry of the system, and $\mathbf{B}_{ij}(\Phi_{ij}, \Phi_{i\ell})$ is an N vector function of $\Phi_{ij}, \Phi_{i\ell}$. When the solutions of (35) have been determined, and we do not include details of the method used, the potentials at any point in Ω may be obtained from (33).

For ϕ_{20} we have a classical interior Neumann problem

$$\mathbf{E}\Phi_{20} = \mathbf{G}\Phi'_{20}, \tag{36}$$

with $\Phi'_{20} = \partial\Phi_{20}/\partial n$ prescribed on $\partial\Omega$. The matrix $\mathbf{E}$ is singular, and as a consequence we have adopted a least-square method of solution as recommended by Jaswon and Symm [10].

The solution domain Ω is, formally, infinite in extent. Accordingly, we must ensure that the boundaries $x = x_\ell, x_r$; $y = y_d$ are sufficiently remote from the cylinder. We note that the disturbance associated with the cylinder and free surface decays rapidly with depth. To take advantage of this in our computational scheme we have allowed the length of the boundary element $\partial\Omega^m$ to increase with depth, and used fewer elements per unit length on $y = y_d$ than that on $y = h$. This allows us, for a given computational effort, to have a relatively large number of elements at the free surface $y = h$, and on the cylinder, where we expect the most rapid variation in flow properties. In the next section, for a particular case, we consider the effect of varying these quantities.

We note, finally, that when the potentials ϕ_{ij} have been determined the corresponding stream functions ψ_{ij} may be obtained from the Cauchy-Riemann equations.

4. Results and discussion

Results have been obtained for various values of the wave number k and cylinder depth h. Emphasis is placed on smaller values of k and h. The closer the cylinder to the free surface, the greater the disturbance it makes to the flow.

Before discussing our results in any detail, we make a comparison for a particular case, namely $k = 0.56$, $\epsilon = 0.16$ and $h = 1.5$ at $t = 0$ for which results have been obtained by Vada [4]. The results we obtain for comparison are for five different cases, corresponding to different values of x_ℓ, x_r, y_d and N. These different cases are delineated in Table 1.

We note that N_1 denotes the number of elements $\partial\Omega$ on the cylinder, N_2 on $y = y_d$, N_3 on $x = x_\ell$, N_4 on $y = h$ and N_5 on $x = x_r$, with $N = \sum_i N_i$. In Figure 2 we show the free-surface shape as calculated from these five cases, and also include the result taken from Vada [4]. As we see, it is not possible to distinguish graphically between these various cases. In particular we note that the values of η at $x = x_\ell, x = x_r$ for cases 1, 2 and 3 compare very well with the values at these points when the larger solution domains, cases 4 and 5, are used.

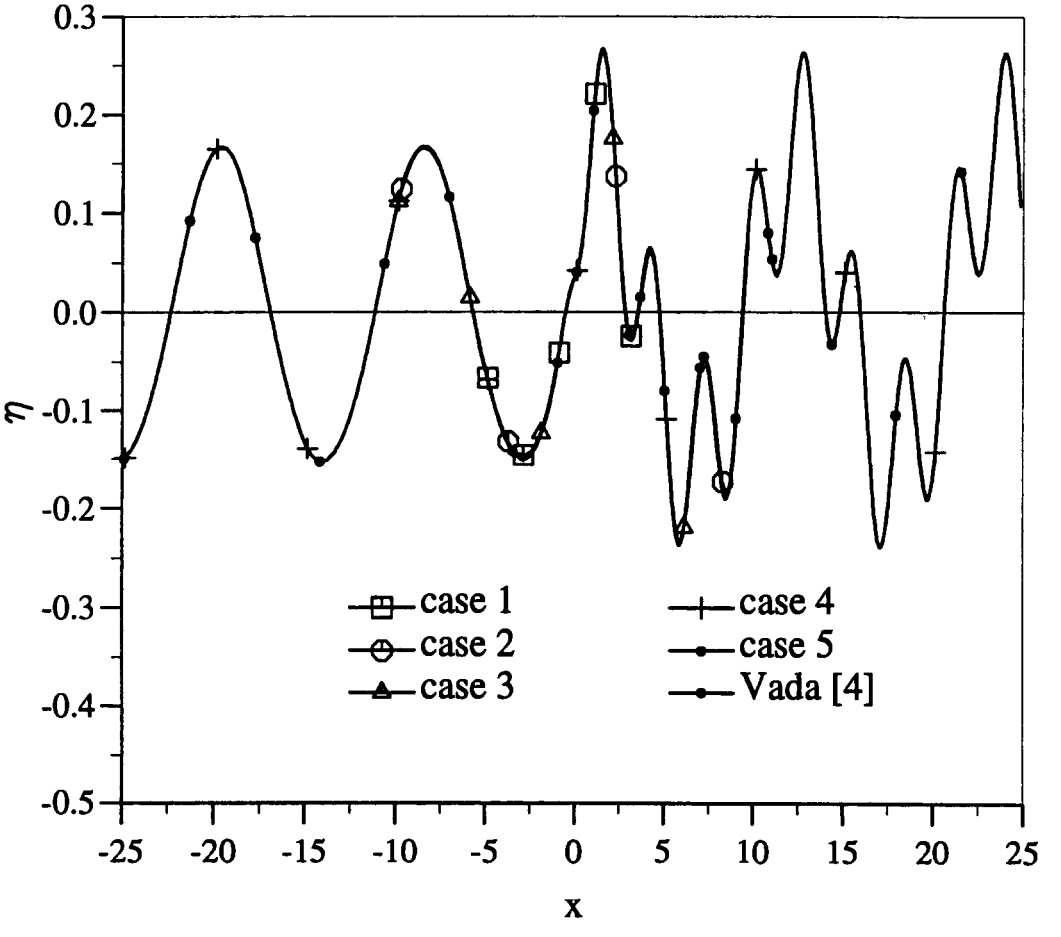

Figure 2. Comparison of the free surface wave with that obtained by Vada [4].

Table 1. Testing parameters for $k = 0.56$, $\epsilon = 0.16$ and $h = 1.5$.

Case No	x_l	x_r	y_d	N_1	N_2	N_3	N_4	N_5
1	−5	5	−50	80	30	80	100	80
2	−10	10	−50	80	60	80	100	80
3	−10	10	−50	120	80	100	200	100
4	−25	25	−100	80	100	100	500	100
5	−25	25	−100	120	100	120	700	120

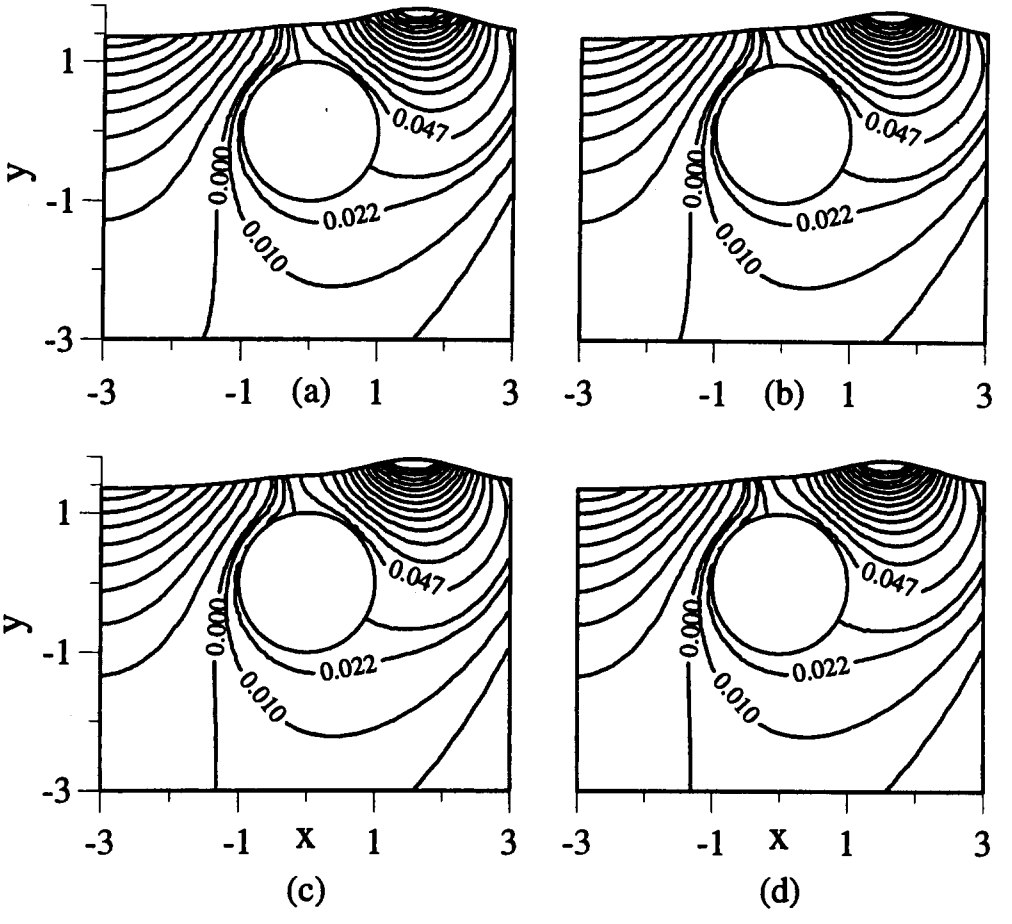

Figure 3. The instantaneous streamlines at $t = 0$ for different sizes of mesh and solution domain as listed in Table 1. (a) case 2, (b) case 3, (c) case 4, (d) case 5.

Further details of the flow field are displayed in Figure 3. There we show the instantaneous streamlines at time $t = 0$ for this same test problem, as calculated from cases 2 to 5 listed in Table 1. In these diagrams all terms up to $O(\epsilon^2)$ have been included as shown in (5), (10) and (11). Between the free surface and the streamlines $\psi = 0, 0.047$ the increment in stream function on the streamlines shown is 0.025. As is evident, the results from the different configurations and mesh sizes are indistinguishable graphically. This suggests that our method gives good accuracy for relatively small solution domains and large mesh sizes. A further check on the accuracy of our results is the second-order reflection coefficient R_2. For the test

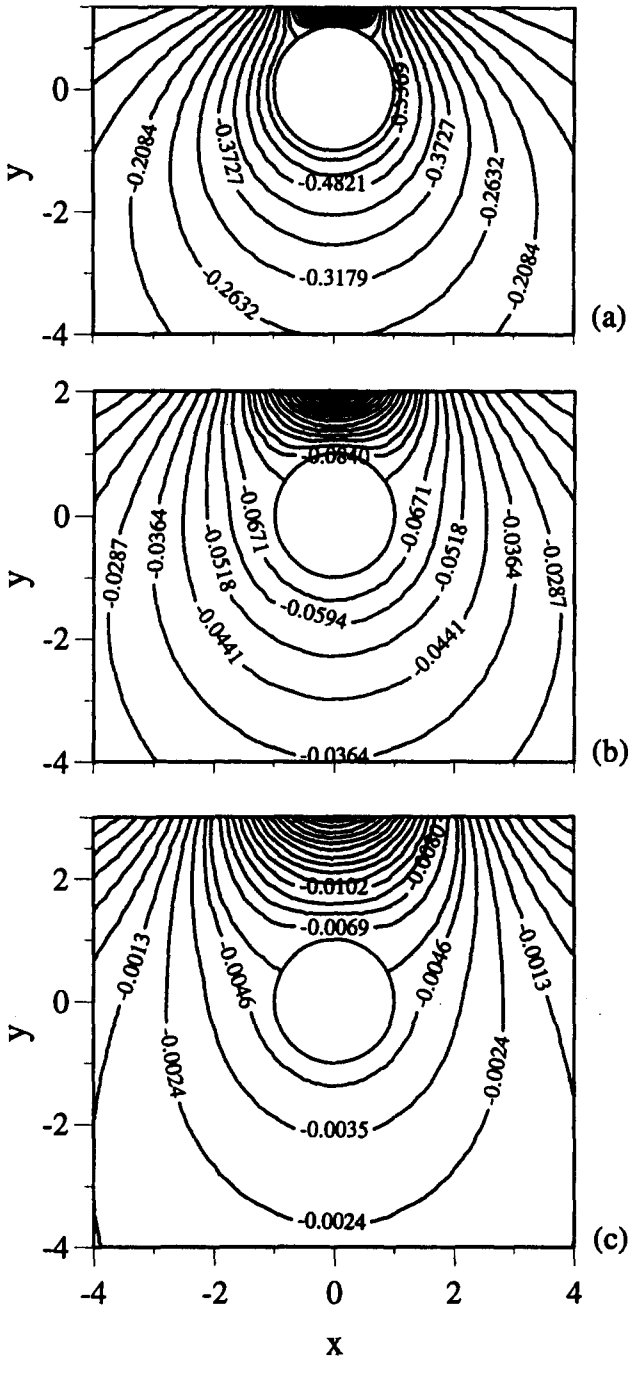

Figure 4. The time-averaged streamlines for $k = 0.5$. (a) $h = 1.3$, (b) $h = 2$, (c) $h = 3$.

case reported here Vada [4] estimated $R_2 = O(10^{-2})$ and suggested that, in fact, this may well be zero as is the first-order reflection coefficient. Subsequently McIver and McIver [6] demonstrated that, indeed, $R_2 \equiv 0$. For all of the results we describe below we have calculated the reflection coefficient R_2 in the manner indicated by McIver and McIver, which involves

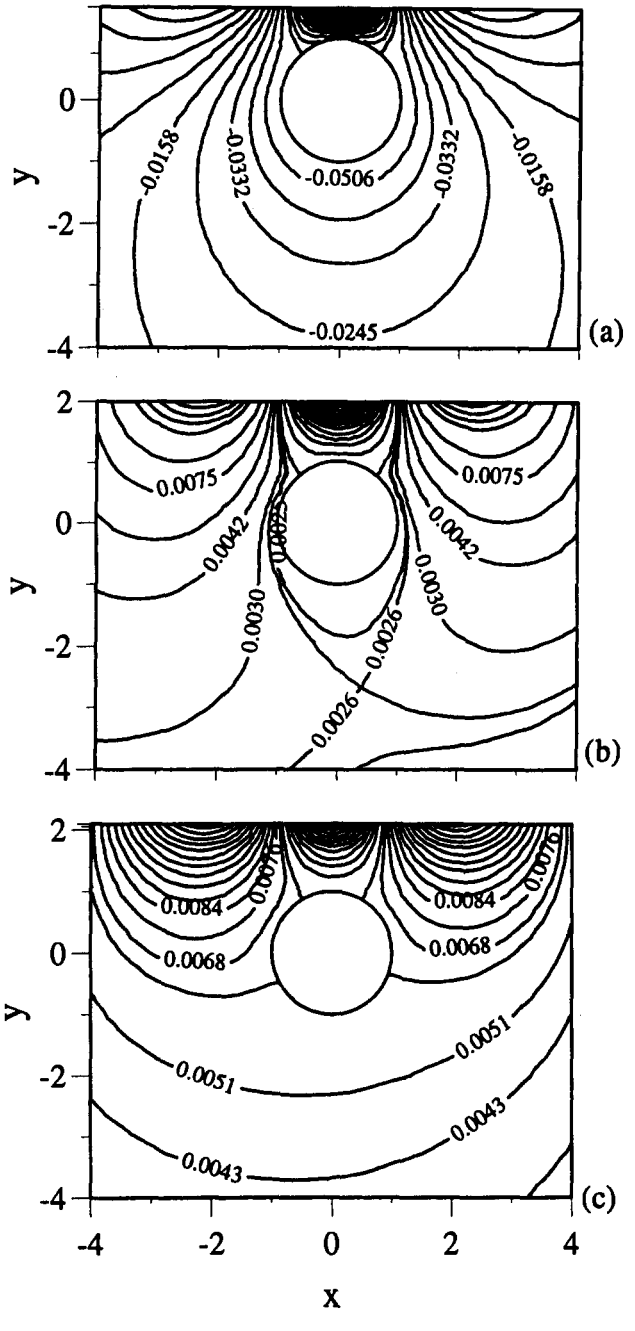

Figure 5a. The time-averaged streamlines for $k = 1$. (a) $h = 1.5$, (b) $h = 1.95$, (c) $h = 2.1$, (d) $h = 2.3$, (e) $h = 3$.

an integral over the free surface of products of first-order quantities as in (17) and (18). In all the cases we consider $R_2 = O(10^{-3})$.

The above discussion gives confidence in the effectiveness of our method of solution. We now concentrate on the second-order solution, and in particular upon that part represented by the potential ϕ_{20}. We refer to this as the streaming, or steady streaming, motion and we

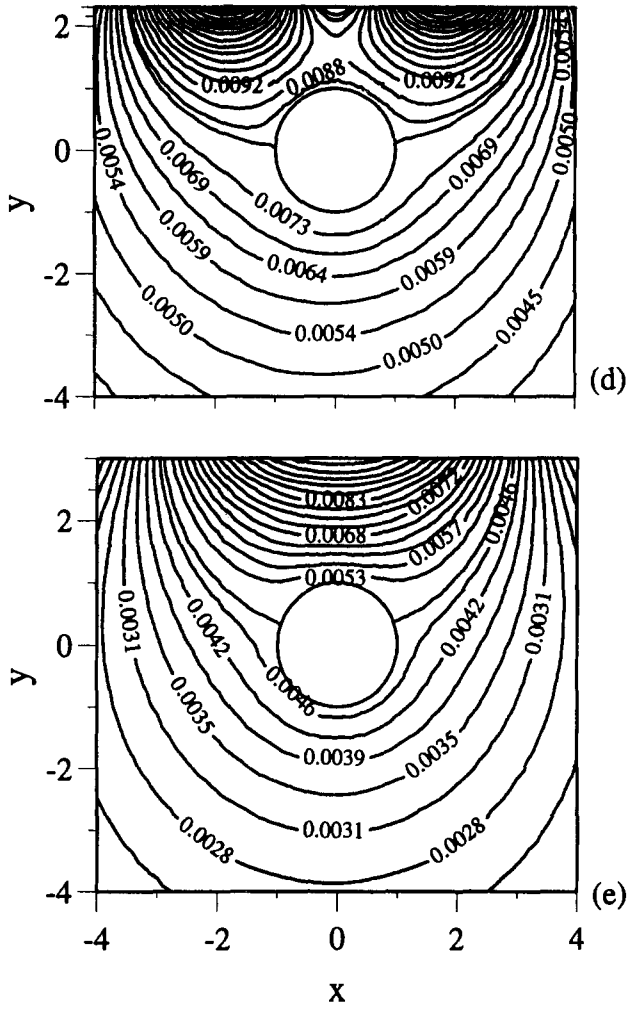

Figure 5b.

note that it does, in fact represent the inviscid time-averaged fluid motion up to second order. This streaming motion is not unique. It is devoid of circulation about the cylinder, but to it we can add a circulatory flow due to a bound vortex within the cylinder. We know from the work of Chaplin [3], [11] that viscous effects within a thin boundary layer adjacent to the cylinder will result in a circulation about it. In a subsequent paper [12] we develop a theory for high-Reynolds number viscous flow that is based on the results presented here. This includes a unique determination of the circulation, and a corresponding potential that augments ϕ_{20}. We show that the introduction of this circulation affects the free-surface displacement (6) only at $O(\epsilon^3)$. In all the solutions we have obtained we have fixed $y_d = -150$, which is clearly adequate as a simulation of infinite depth. As we have seen in Figures 2 and 3, the effect of the presence of the cylinder on the flow is greater on the leeward side than on the side of the incident wave. As a consequence, depending upon the values of k, we have chosen x_ℓ in the range -30 to -20, with x_r in the range 25 to 35. The mesh size at the free surface varies from 0.05 to 0.1 with the number of elements increasing as k increases. At least 40 elements per wavelength were employed. At $x = x_\ell, x_r$ the mesh size close to the free surface

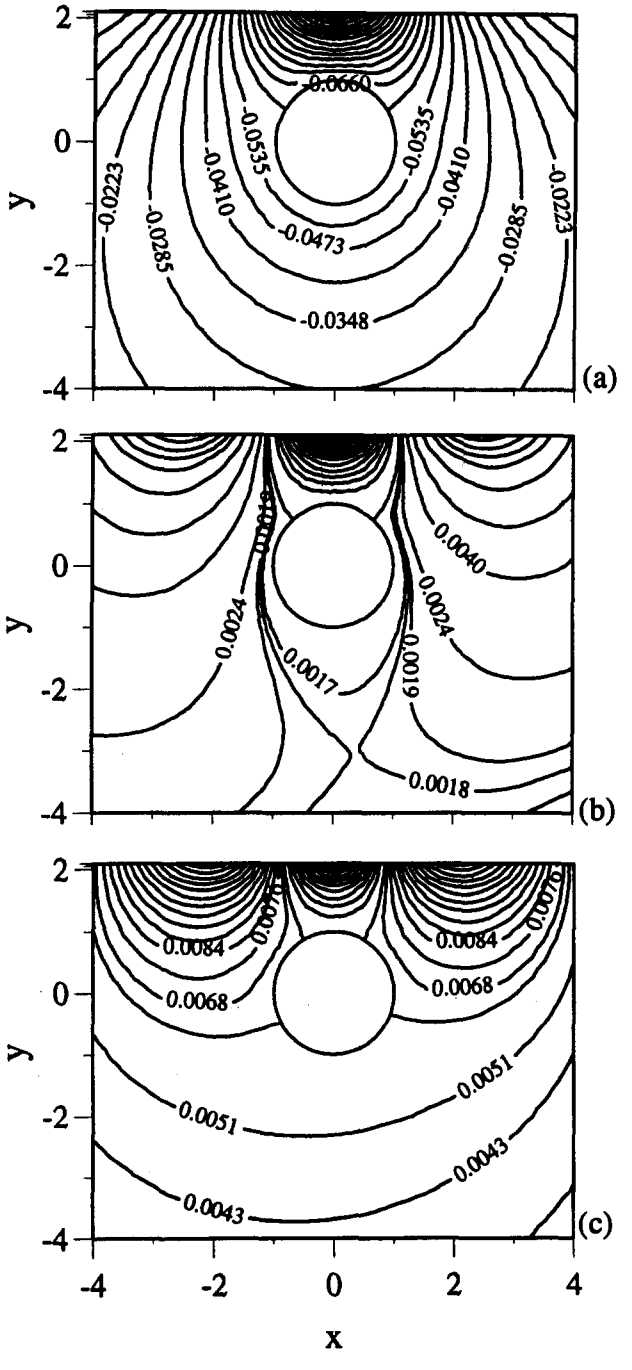

Figure 6a. The time-averaged streamlines for $h = 2.1$. (a) $k = 0.5$, (b) $k = 0.9$, (c) $k = 1$, (d) $k = 1.2$, (e) $k = 2$.

is comparable with that along the free surface, but, as we have already indicated, this increases with increasing depth. At $y = y_d$ a constant mesh size of 0.4 was used in all situations, whilst between 100 and 120 elements were used on the surface of the cylinder.

We have obtained results for $1.3 \leq h \leq 4$ and $0.3 \leq k \leq 3$. Typically, the strongest streaming motion occurs in the region between the cylinder and the free surface. As a first example we show, in Figure 4, the time-averaged streamlines, ψ_{20} = constant, with $k = 0.5$

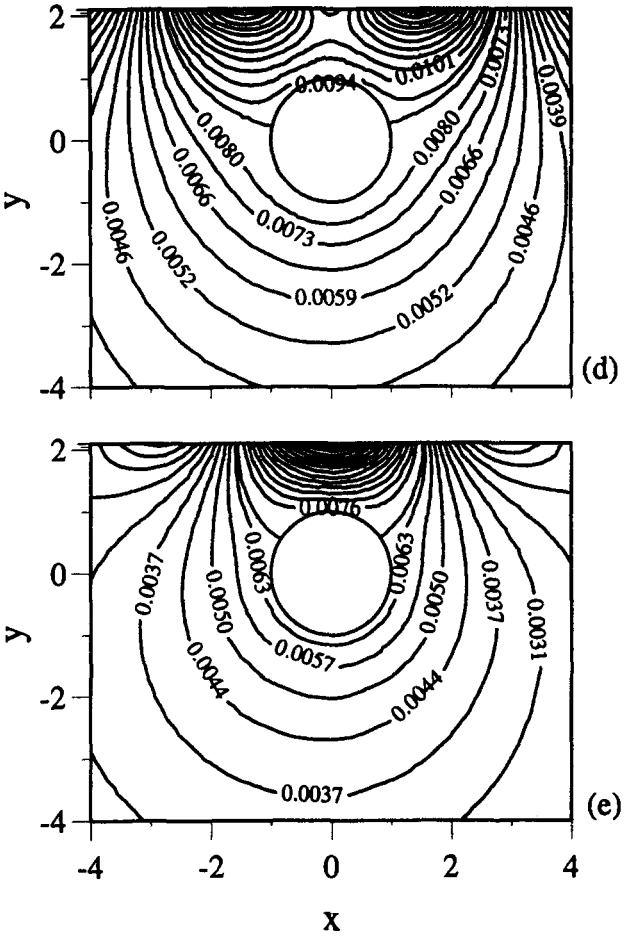

Figure 6b.

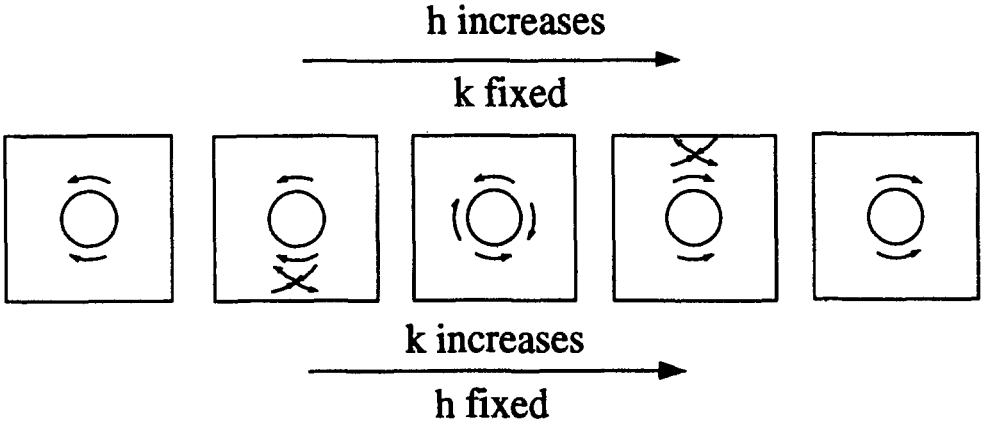

Figure 7. A schematic diagram of the local time-averaged flow direction for fixed $k(h)$ as $h(k)$ increases.

for $h = 1.3, 2$ and 3, successively. There is no qualitative change in the streamline pattern as h increases, although increasing depth brings about a reduction in the streaming strength, as may be expected. In all cases shown in Figure 4 there are two stagnation points on the

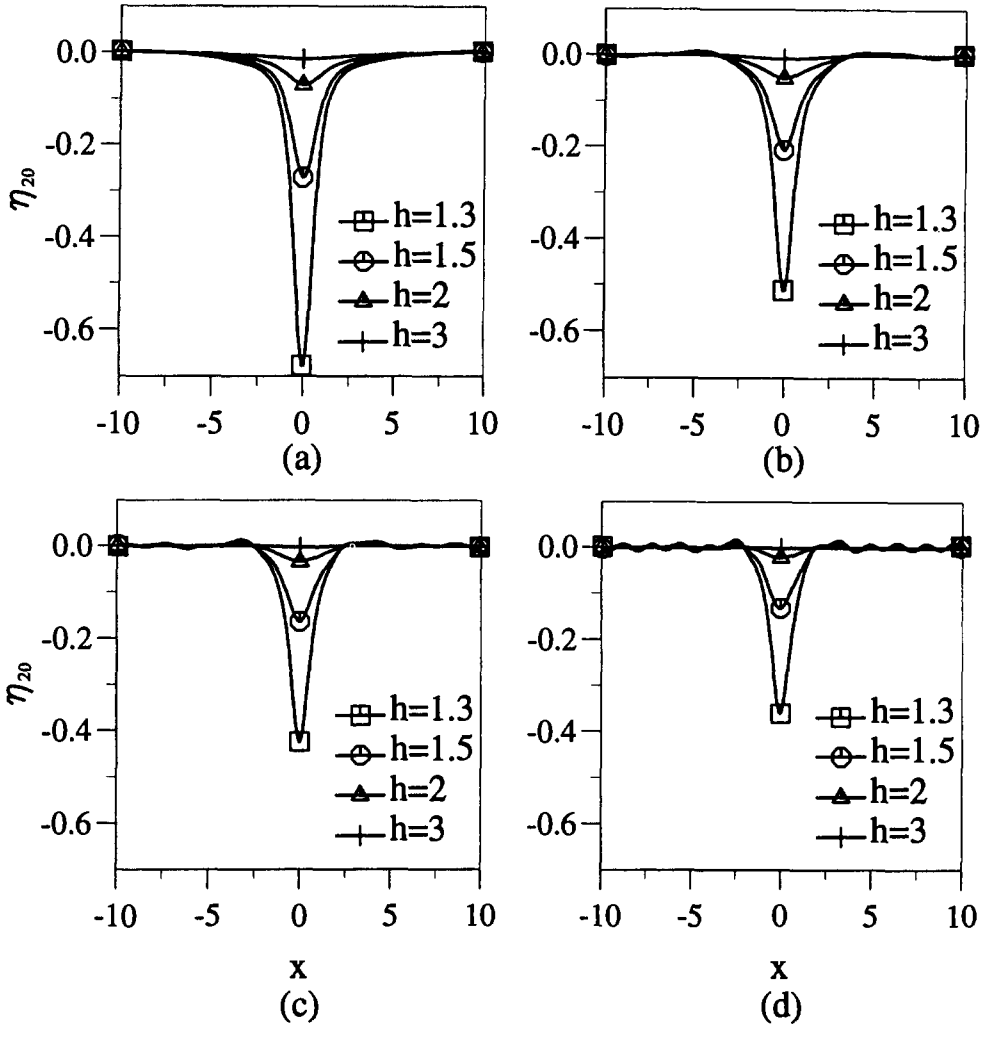

Figure 8. The time-averaged free surface profile η_{20} as a function of k and h. (a) $k = 0.5$, (b) $k = 1$, (c) $k = 1.5$, (d) $k = 2$.

cylinder, and at the highest and lowest points on the cylinder the flow is in the direction of x decreasing.

Consider next the results shown in Figure 5 where values of h used are 1.5, 1.95, 2.1, 2.3, 3 and $k = 1$. With the cylinder close to the free surface the time-averaged flow is similar to those shown in Figure 4. However, as the depth increases, a stagnation point in the flow below the cylinder moves close to it, eventually becoming attached and bifurcating, so that there is a range of depth for which there are four stagnation points on the cylinder. As the depth increases further, the upper two stagnation points move together, coalesce, with further depth increase this detaches from the cylinder and moves towards the free surface where it eventually disappears. The flow at the highest and lowest points on the cylinder is now in the direction of x increasing. This same sequence of events, leading to the same qualitative change in the flow in the neighbourhood of the cylinder, is observed when the cylinder depth is fixed and the wavenumber increases as we see in Figure 6 in the case of $h = 2.1$ for example.

Qualitative changes in the flow close to the cylinder, as discussed in relation to Figures 5 and 6, are summarised schematically in Figure 7.

We turn next to the free surface displacement. Since the reflection coefficients $R_1 = R_2 = 0$, there is little modification to the incident wave profile in $x < 0$, but with a quite different situation when the wave has passed over the cylinder, as is clearly shown in Figure 2. However, the time-averaged component of this, represented by η_{20} in equation (30), is largely confined to the neighborhood of the cylinder. On average, the free surface is depressed over the cylinder, a form of 'set-down'. The degree of depression depends, in particular, upon the depth of the cylinder, decreasing as the depth increases. For a given cylinder depth the free-surface depression also decreases as the wavenumber increases. Figure 8 shows these features for a range of depths and wave numbers.

5. Conclusions

In this paper we have considered the flow induced by the propagation of waves on the surface of an inviscid, incompressible fluid over a submerged circular cylinder. We have completed the solution up to second order in the wave amplitude including, in particular, the time-independent part of the second-order solution that allows the time-averaged flow to be considered. We have shown how the flow pattern in the neighbourhood of the cylinder changes, qualitatively, with variations in the cylinder depth and wave number.

Acknowledgement

The authors are indebted to Dr Maureen McIver for helpful discussions and comments.

References

1. W.R. Dean, On the reflexion of surface waves by a submerged circular cylinder. *Proc. Camb. Phil. Soc.* 44 (1948) 483–491.
2. F. Ursell, Surface waves on deep water in the presence of a submerged circular cylinder. I. *Proc. Camb. Phil. Soc.* 46 (1950) 141–152.
3. J.R. Chaplin, Mass transport around a horizontal cylinder beneath waves. *J. Fluid Mech.* 140 (1984) 175–187.
4. T.A. Vada, A numerical solution of the second-order wave-diffraction problem for a submerged cylinder of arbitrary shape. *J. Fluid. Mech.* 174 (1987) 23–37.
5. J.V. Wehausen and E.V. Laitone, 'Surface waves'. In S. Flügge, ed., *Encyclopedia of Physics, Volume IX, Fluid Dynamics III*, Springer-Verlag, (1960).
6. M. McIver and P. McIver, Second-order wave diffraction by a submerged circular cylinder. *J. Fluid Mech.* 219 (1990) 519–529.
7. G.X. Wu, On the second-order wave reflection and transmission by a horizontal cylinder. *Appl. Ocean Res.* 13 (1991) 58–62.
8. J.R. Chaplin, Nonlinear forces on a horizontal cylinder beneath waves. *J. Fluid Mech.* 147 (1984) 449–464.
9. R.W. Yeung, Numerical methods in free-surface flows. *Ann. Rev. Fluid Mech.* 14 (1982) 395–442.
10. M.A. Jaswon and G.T. Symm, *Integral Equation Methods in Potential Theory and Elastostatics*, Academic Press, London, (1977).
11. J.R. Chaplin, Orbital flow around a circular cylinder. Part I. Steady streaming in non-uniform conditions. *J. Fluid Mech.* 237 (1992) 395–411.
12. B. Yan and N. Riley, Boundary layer flow around a submerged circular cylinder induced by free-surface travelling waves. *J. Fluid Mech.* (to be published) 1996.